

**Conversion of CO₂ to Epoxides or Oxazolidinones enabled
by Mixed-Valence Cu^I/Cu^{II}-Organic Framework
Constructed by Tri-functional Linker**

Ao-gang Liu,^a Yuan Chen,^a Peng-da Liu,^a Wei Qi,^{a,*} Bao Li^{a,*}

^a Key Laboratory of Material Chemistry for Energy Conversion and Storage,
Semiconductor chemistry center, School of Chemistry and Chemical Engineering,
Hubei Key Laboratory of Bioinorganic Chemistry&Materia Medica, Huazhong
University of Science and Technology, Wuhan, Hubei 430074, People's Republic of
China. Email: qiwei@hust.edu.cn; libao@hust.edu.cn

Experimental section

Materials and methods.

All starting chemicals were purchased from commercial sources and were used without further purification. The starting materials, tri-nuclear Fe_3O and hexacarboxyl ligands, had been synthesized according to the references.^[1,2]

Thermogravimetric analysis (TGA) was performed on a Perkin-Elmer TG-7 analyzer heated from 25 to 800 °C under nitrogen atmosphere. Powder X-ray diffraction (PXRD) patterns for the as-synthesized samples were recorded on a X-ray diffraction meter (D/max 2500 PC, Rigaku) with $\text{Cu-K}\alpha$ radiation (1.5406 Å). X-ray photoelectron spectroscopy (XPS) was carried out on a VGESCALBMKII X-ray photoelectron system with an Al $\text{K}\alpha$ radiation (1486.6 eV). ^1H NMR spectra was measured on Avance III400MHz.

The synthesis of ligand H_2L

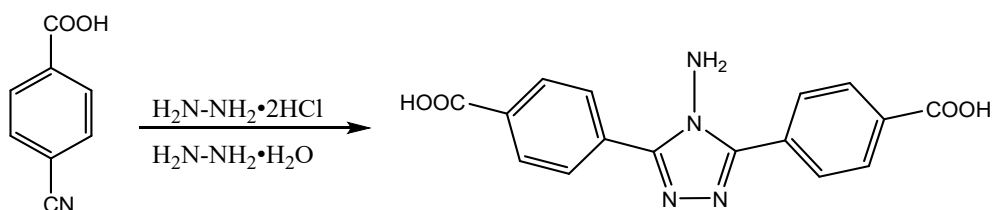


Fig. S1 The synthesis step of triazole dicarboxylic acid ligand

Put 4-cyanobenzoic acid (2.20 g, 15 mmol) and Hydrazine dihydrochloride (2.10 g, 20 mmol) in a 100 mL three-necked flask, evacuate for 10 min and pass argon gas, add 16 mL ethylene glycol and stir well, the solution is white. Add 2.5 mL of hydrazine hydrate slowly while stirring, and the solution gradually becomes colorless. 130 °C oil bath reaction for three days, the solution is milky white. After the reaction, cool slowly to room temperature, add 50 mL of deionized water, stir thoroughly and then filter under reduced pressure, and wash with deionized water several times. After drying, a milky white powder was obtained with a yield of 68.74%. ^1H NMR: 12.81 ppm, 8.20 ppm, 8.12 ppm, 6.44 ppm (1:2:2:1).

The synthesis of Cu-MOF

H₂L 22 mg and 20 mg of cuprous iodide were added into a glass vial, 4 mL of N,N-dimethylformamide was slowly added with a pipette, 2 drops of tetrafluoroboric acid was added after ultrasonic homogenization, stirred well and then put into a polytetrafluoroethylene reactor and placed in an oven at 85 °C for three days, and green cubic crystalline samples were obtained after cooling to room temperature with a yield of about 42%, which were directly utilized as the other characterization and catalyst.

The synthesis of alkynylamine substrates

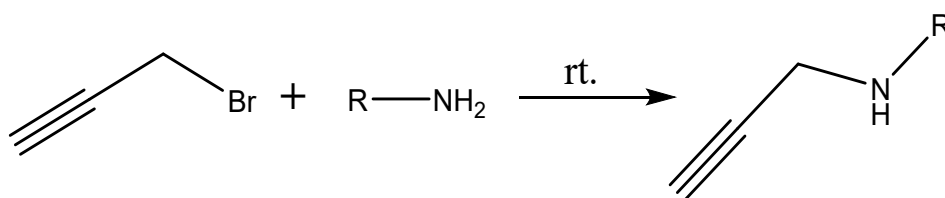


Fig. S2 Preparation of alkynylamine substrates containing different groups

Organic amine (162 mmol) with different substituent was put into a 100 mL round bottom flask and bromopropyne (27 mmol) was slowly added dropwise into it under the condition of ice water bath, stirred for 30 min, then slowly raised to room temperature and reacted at room temperature overnight. At the end of the reaction, 20 mL of ether was added to the obtained solution and diluted, and then extracted three times with 20 mL of saturated NaHCO₃. The collected organic phase was dried with anhydrous Na₂SO₄, filtered and then the solution was concentrated under reduced pressure and separated by a chromatographic column to finally obtain the oily liquid product. Benzylamine, β -phenylethylamine, cyclohexylamine and isopropylamine with different substituents were prepared by the same method.

X-Ray Structural Determination

Diffraction data for Cu-MOF (HUST-23) (0.3 × 0.2 × 0.2 mm) was collected via Bruker Venture using Cu-K α ($\lambda = 1.54178 \text{ \AA}$) radiation at 100 K. The structures of complexes were solved by direct methods, and the non-hydrogen atoms were located from the trial structure and then refined anisotropically with SHELXTL using a full-

matrix leastsquares procedure based on F^2 values. The hydrogen atom positions were fixed geometrically at calculated distances and allowed to ride on the parent atoms. Attempts to define the highly disordered solvent molecules were unsuccessful, so the structure was refined with the PLATON “SQUEEZE” procedure. CCDC-2174292 for the data under different temperature contain the supplementary crystallographic data for this paper. These data can be obtained free of charge from The Cambridge Crystallographic Data Centre via <http://www.ccdc.cam.ac.uk/datarequest/cif>.

The related catalytic experiments with CO₂

Before the catalysis experiments, Cu-MOF was soaked in CH₃CN, and fresh CH₃CN was changed every 12 hours, and soaked for three days. Then filtered and dried at 60 °C to remove the solvent molecules. In a general experiment, 0.057 mmol catalyst based on Cu and 1.3 mmol substrate were added to a glass reaction tube with a CO₂ balloon and sealed the reactor. Subsequently, placed the glass reaction tube in a water bath at 30 °C and stirred magnetically for 1 h. After the reaction, the catalyst was separated by centrifugation, and the mixed solution after the reaction with 1,3,5-trimethoxybenzene as the internal standard was analyzed by ¹H NMR.

The cycling catalytic experiments with CO₂

Before the catalysis experiments, Cu-MOF was soaked in CH₃CN, and fresh CH₃CN was changed every 12 hours, and soaked for three days. Then filtered and dried at 60 °C to remove the solvent molecules. In a general experiment, 0.057 mmol catalyst based on Cu and 1.3 mmol substrate were added to a glass reaction tube with a CO₂ balloon and sealed the reactor. Subsequently, placed the glass reaction tube in a water bath at 30 °C and stirred magnetically for 1 h. After 1 hour, the mixture in the tube was separated by centrifugation, and the liquid was calculated the product yield by ¹H NMR, and the solid was transferred to a new tube. Then, the next cycle of experiments was operated as the initial run. As Figure S13 shown, the catalyst can be recycled at least five times and its catalytic activity is not significantly reduced. The little reduction of the reaction yield was caused by the loss of small amounts of the

catalyst.

Table S1 Crystal parameters of Cu-MOF

Empirical formula	C ₃₈ H ₃₈ Cu ₆ I ₄ N ₁₀ O ₁₂
Formula weight	1715.69
Temperature/K	100
Crystal system	trigonal
Space group	<i>R</i> -3 <i>c</i>
<i>a</i> /Å	35.9116(4)
<i>b</i> /Å	35.9116(4)
<i>c</i> /Å	87.2194(16)
<i>α</i> /°	90
<i>β</i> /°	90
<i>γ</i> /°	120
Volume/Å ³	97412(3)
<i>Z</i>	36
$\rho_{\text{calc}}/\text{cm}^3$	1.029
μ/mm^{-1}	10.511
<i>F</i> (000)	28081.0
Crystal size/mm ³	0.3 × 0.2 × 0.2
Radiation	CuK α (λ = 1.54184)
2 θ range for data collection/°	4.922 to 145.318
Reflections collected	21330
Independent reflections	21330 [<i>R</i> _{int} = 0.0701, <i>R</i> _{sigma} = 0.0323]
Data/restraints/parameters	21330/0/639
Goodness-of-fit on <i>F</i> ²	1.052
Final <i>R</i> indexes [<i>I</i> ≥ 2 σ (<i>I</i>)]	<i>R</i> ₁ = 0.0701, <i>wR</i> ₂ = 0.1978
Final <i>R</i> indexes [all data]	<i>R</i> ₁ = 0.0781, <i>wR</i> ₂ = 0.2056
Largest diff. peak/hole / e Å ⁻³	3.36/-1.79

Table S2 The selected bond length of Cu-MOF

Atom	Atom	Length/Å	Atom	Atom	Length/Å
I1	Cu4	2.5917(10)	N7	N6	1.380(7)
I1	Cu3	2.5782(12)	N2	N3	1.384(7)

Atom	Atom	Length/Å	Atom	Atom	Length/Å
I2	Cu4	2.7829(12)	N1	N4	1.420(9)
I2	Cu3	2.6476(12)	Cu1	Cu1 ⁴	2.6243(15)
I2	Cu2	2.6898(13)	Cu1	O4 ⁴	1.967(4)
I3	Cu4	2.7251(12)	Cu1	O2 ⁵	1.956(4)
I3	Cu2	2.7367(14)	Cu1	O1 ⁶	1.947(4)
I3	Cu5	2.6488(17)	Cu1	O3	1.939(4)
I4	Cu2	2.6340(11)	Cu1	O12	2.119(4)
I4	Cu5	2.5245(16)	Cu4	Cu3	2.5761(14)
Cu6	Cu6 ¹	2.6136(16)	Cu4	Cu2	2.8225(14)
Cu6	O5 ²	1.954(4)	Cu4	N6	2.032(6)
Cu6	O6 ³	1.962(4)	Cu3	N2	2.033(6)
Cu6	O8	1.947(4)	Cu2	Cu5	2.5824(19)
Cu6	O7 ¹	1.968(4)	Cu2	N3	2.017(6)
Cu6	O10	2.106(5)	Cu5	N7	2.009(6)
Cu3	O11	2.096(6)	Cu5	O9	2.429(6)
O5	Cu6 ⁷	1.954(4)	O2	Cu1 ⁹	1.955(4)
O5	C24	1.259(7)	O1	Cu1 ¹⁰	1.947(4)
O6	Cu6 ⁸	1.962(4)	O7	Cu6 ¹	1.968(4)
O4	Cu1 ⁴	1.967(4)	N5	N8	1.417(9)

Symmetry code: ¹1/3-Y+X, 2/3-Y, 7/6-Z; ²-2/3+Y, -1/3+X, 7/6-Z; ³+Y-X, 1-X, +Z; ⁴2/3-X, 1/3-Y, 4/3-Z; ⁵-1/3+Y, 1/3-X+Y, 4/3-Z; ⁶1-Y, +X-Y, +Z; ⁷1/3+Y, 2/3+X, 7/6-Z; ⁸1-Y, 1+X-Y, +Z; ⁹2/3-Y+X, 1/3+X, 4/3-Z; ¹⁰1+Y-X, 1-X, +Z

Table S3 Selected bond angle of Cu-MOF

Atom	Atom	Atom	Angle/°	Atom	Atom	Atom	Angle/°
Cu3	I1	Cu4	59.77(3)	N6	N7	Cu5	117.0(4)
Cu3	I2	Cu4	56.57(3)	N7	N6	Cu4	116.5(4)
Cu3	I2	Cu2	76.02(3)	N3	N2	Cu3	119.6(5)
Cu2	I2	Cu4	62.07(3)	N2	N3	Cu2	116.3(4)
Cu4	I3	Cu2	62.23(3)	N3	Cu2	I4	128.78(15)
Cu5	I3	Cu4	73.11(4)	N3	Cu2	Cu4	104.11(15)
Cu5	I3	Cu2	57.28(5)	N3	Cu2	Cu5	153.9(2)

Atom	Atom	Atom	Angle/°	Atom	Atom	Atom	Angle/°
Cu5	I4	Cu2	60.04(4)	O3	Cu1	O1 ⁶	87.8(2)
O5 ¹	Cu6	Cu6 ²	84.04(13)	O3	Cu1	O12	100.2(2)
O5 ¹	Cu6	O6 ³	88.67(19)	O12	Cu1	Cu1 ⁴	172.82(14)
O5 ¹	Cu6	O7 ²	89.28(19)	I1	Cu4	I2	111.35(4)
O5 ¹	Cu6	O10	93.90(19)	I1	Cu4	I3	108.93(4)
O6 ³	Cu6	Cu6 ²	84.62(13)	I1	Cu4	Cu2	127.43(5)
O6 ³	Cu6	O7 ²	168.73(19)	I2	Cu4	Cu2	57.35(4)
O6 ³	Cu6	O10	97.6(2)	I3	Cu4	I2	116.32(4)
O8	Cu6	Cu6 ²	84.08(13)	I3	Cu4	Cu2	59.09(3)
O8	Cu6	O5 ¹	168.04(19)	Cu3	Cu4	I1	59.85(3)
O8	Cu6	O6 ³	88.89(18)	Cu3	Cu4	I2	59.06(4)
O8	Cu6	O7 ²	90.84(18)	Cu3	Cu4	I3	107.34(4)
O8	Cu6	O10	98.02(19)	Cu3	Cu4	Cu2	74.86(4)
O7 ²	Cu6	Cu6 ²	84.15(14)	N6	Cu4	I1	125.21(14)
O7 ²	Cu6	O10	93.6(2)	N6	Cu4	I2	93.02(18)
O10	Cu6	Cu6 ²	176.92(15)	N6	Cu4	I3	101.66(17)
O4 ⁴	Cu1	Cu1 ⁴	82.04(14)	N6	Cu4	Cu3	146.40(19)
O4 ⁴	Cu1	O12	91.8(2)	N6	Cu4	Cu2	107.20(14)
O2 ⁵	Cu1	Cu1 ⁴	83.37(14)	I1	Cu3	I2	116.33(4)
O2 ⁵	Cu1	O4 ⁴	88.9(2)	Cu4	Cu3	I1	60.37(3)
O2 ⁵	Cu1	O12	92.79(19)	Cu4	Cu3	I2	64.36(4)
O1 ⁶	Cu1	Cu1 ⁴	84.87(14)	N2	Cu3	I1	121.59(19)
O1 ⁶	Cu1	O4 ⁴	90.2(2)	N2	Cu3	I2	102.34(16)
O1 ⁶	Cu1	O2 ⁵	168.2(2)	N2	Cu3	Cu4	106.98(17)
O1 ⁶	Cu1	O12	98.98(19)	N2	Cu3	O11	102.4(3)
O3	Cu1	Cu1 ⁴	85.99(14)	O11	Cu3	I1	108.0(2)
O3	Cu1	O4 ⁴	168.00(19)	O11	Cu3	I2	104.1(2)
O3	Cu1	O2 ⁵	90.7(2)	O11	Cu3	Cu4	150.1(2)
I4	Cu5	I3	111.05(5)	I4	Cu2	Cu4	126.82(5)
I4	Cu5	Cu2	62.09(4)	Cu5	Cu2	I2	98.80(5)
Cu2	Cu5	I3	63.07(4)	Cu5	Cu2	I3	59.65(5)

Atom	Atom	Atom	Angle/°	Atom	Atom	Atom	Angle/°
N7	Cu5	I3	104.56(17)	Cu5	Cu2	I4	57.88(4)
N7	Cu5	I4	133.4(2)	Cu5	Cu2	Cu4	72.49(4)
N7	Cu5	Cu2	112.97(17)	N3	Cu2	I2	101.75(18)
I2	Cu2	I3	119.14(4)	N3	Cu2	I3	95.96(19)
I2	Cu2	Cu4	60.59(3)	N7	Cu5	O9	100.7(2)

Symmetry code: $^1-2/3+Y, -1/3+X, 7/6-Z$; $^21/3-Y+X, 2/3-Y, 7/6-Z$; $^3+Y-X, 1-X, +Z$; $^42/3-X, 1/3-Y, 4/3-Z$; $^5-1/3+Y, 1/3-X+Y, 4/3-Z$; $^61-Y, +X-Y, +Z$; $^71/3+Y, 2/3+X, 7/6-Z$; $^81-Y, 1+X-Y, +Z$; $^92/3-Y+X, 1/3+X, 4/3-Z$; $^{10}1+Y-X, 1-X, +Z$

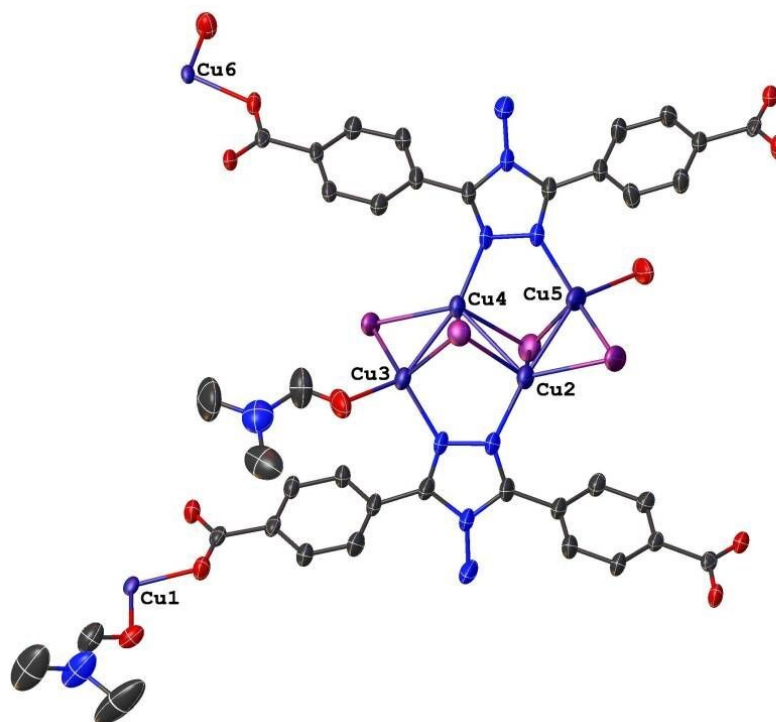


Fig. S1 asymmetric unit of Cu-MOF

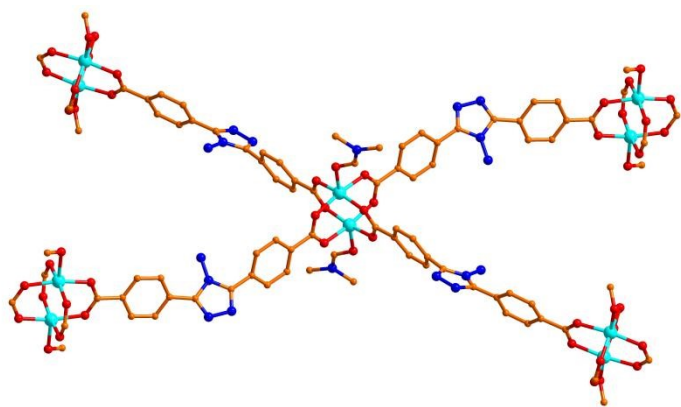


Fig. S2 view of the connection mode of Cu₂ cluster

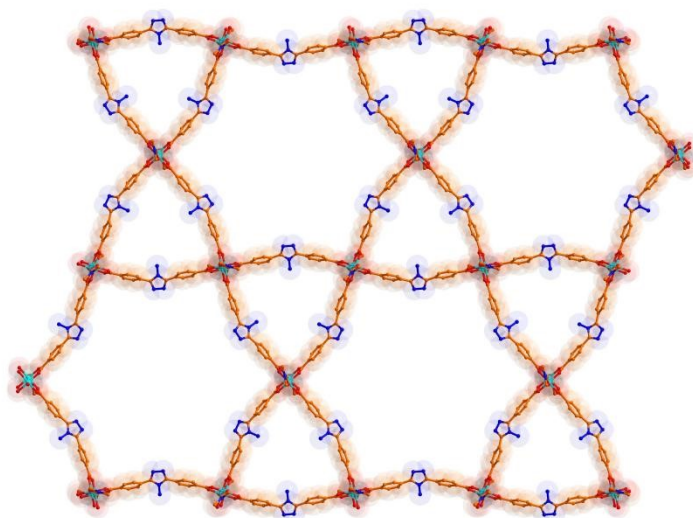


Fig. S3 view of the 2D structure consisting of Cu₂ cluster and ligand

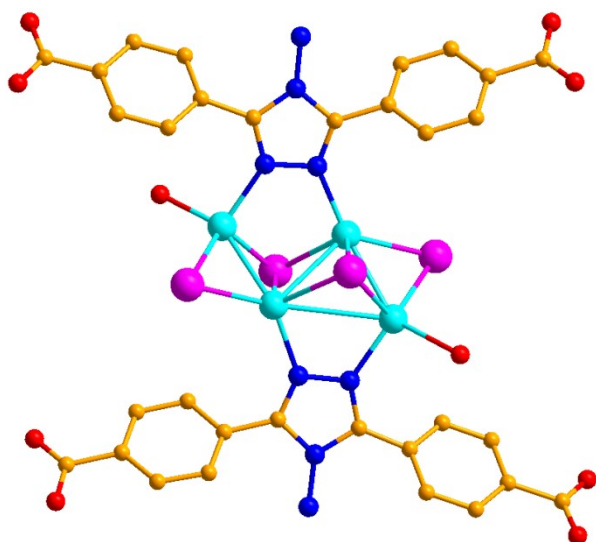


Fig. S4 view of the Cu₄I₄ cluster

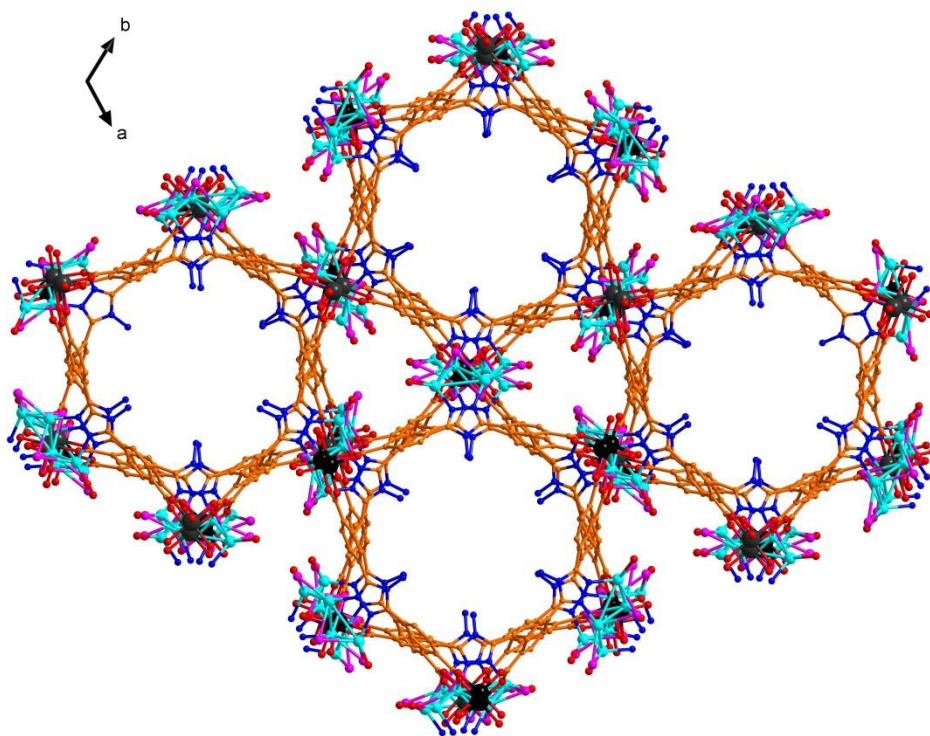


Fig S5. 3D packing mode of Cu-MOF

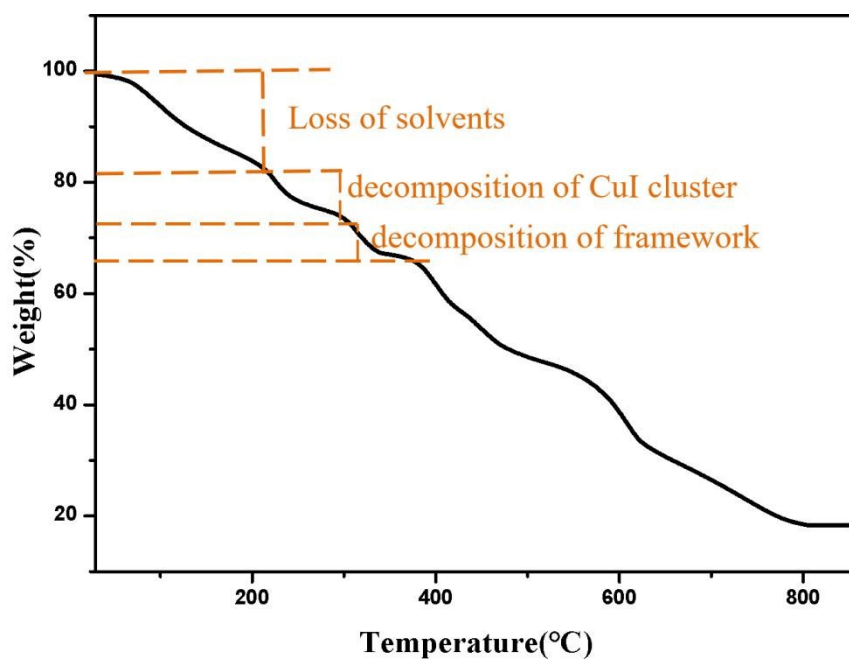


Fig. S6 Thermogravimetric analysis of Cu-MOF

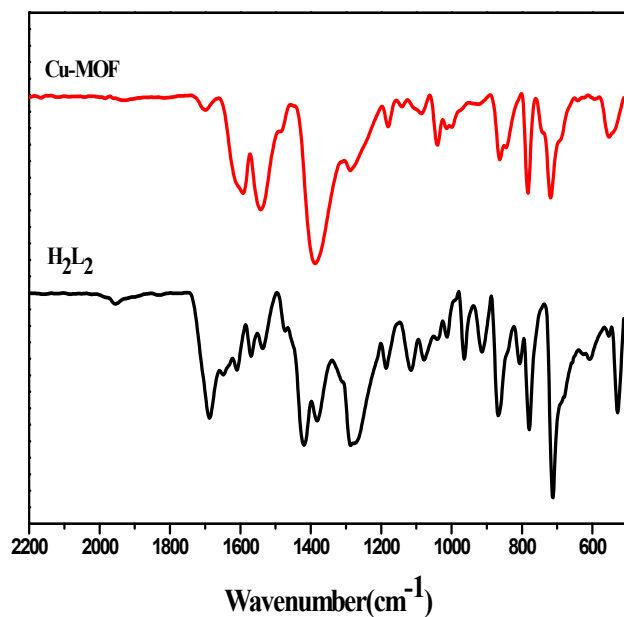


Fig. S7 Infrared contrast of Cu-MOF and triazole dicarboxylic acid ligand

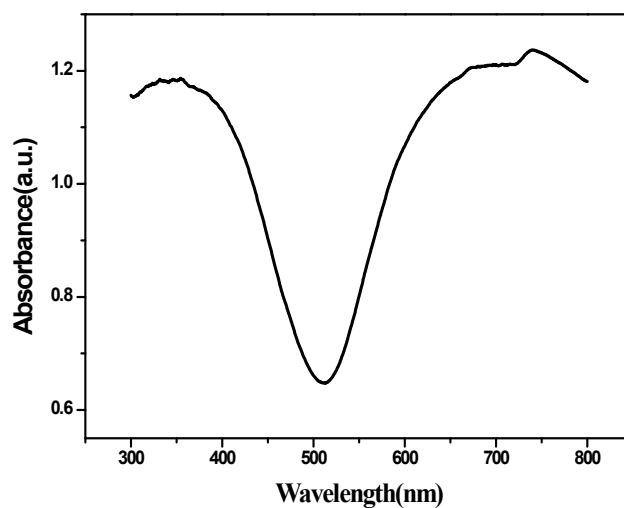


Fig. S8 Solid UV characterization of Cu-MOF

Table S4 Yields of cyclopropenyl carbonate produced under different reaction conditions

Entry	Cu-MOF(% mol)	TBABr (% mol)	T(°C)	t(h)	Yield(%)
1	0.7		25	48	2.3
2		1.0	25	48	21
3	0.7	1.0	25	48	58.5
4	0.7	1.0	25	72	77.5
5	0.7	1.0	30	3	14.5
6	0.7	1.0	30	8	29.2

7	0.7	1.0	30	12	41
8	0.7	1.0	50	3	17.4
9	0.7	1.0	50	8	37.5
10	0.7	1.0	50	12	50
11	0.7	1.0	90	3	95
12	0.7	1.0	90	5	99

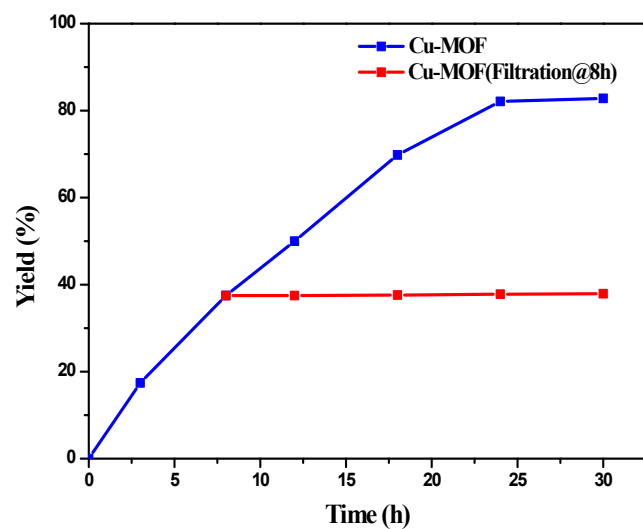


Fig. S9 Comparison of yield of Cu-MOF catalyst before and after 8h filtration

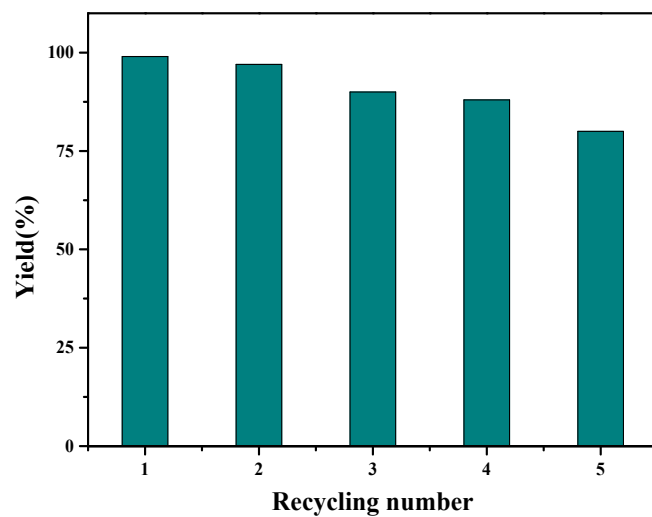


Fig. S10 Cu-MOF cycle number and corresponding yield

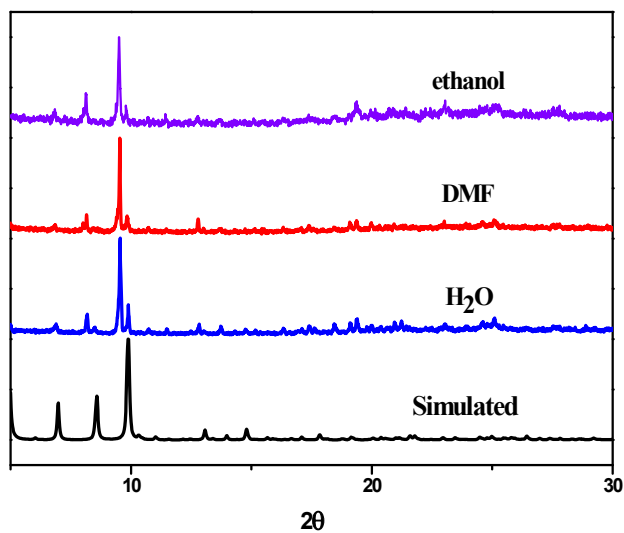


Fig. S11 X-ray powder diffraction characterization of Cu-MOF in different solvents

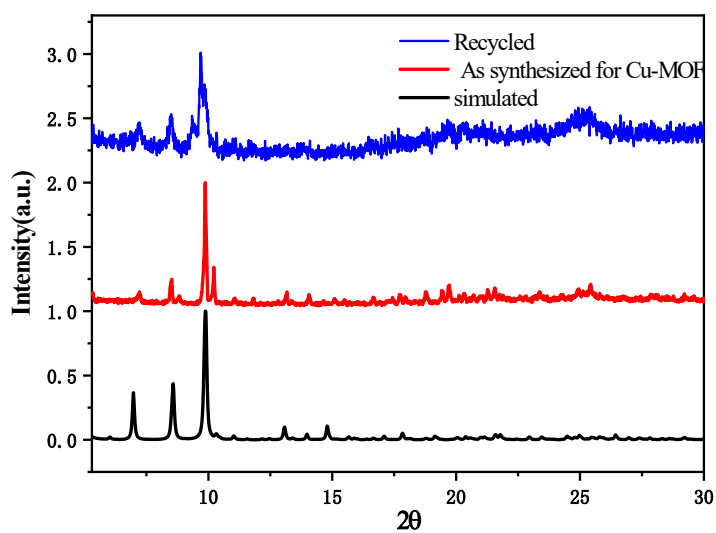


Fig. S12 Comparison of X-ray powder diffraction characterization before and after Cu-MOF participates in catalytic reaction

Table S5 Yield of CO₂ to oxazolidinone with 2-methyl-3-butyne-2-amine under different conditions

Entry	Cu-MOF(mmol)	T(°C)	t(h)	Yield(%)
1	0.28	30	1	45.2
2	0.28	30	3	38.7
3	0.28	30	5	12.9

4	0.28	40	1	40.4
5	0.28	40	3	32.3
6	0.28	40	5	29
7	0.28	40	8	28.2
8	0.28	50	1	59.7
9	0.28	50	3	51.6
10	0.28	60	1	69.4
11	0.28	60	3	58.1

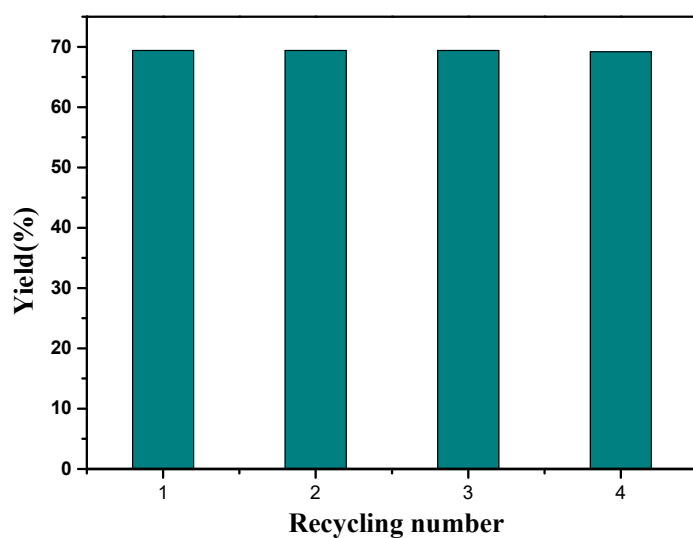


Fig. S13 Cu-MOF cycle number and corresponding yield

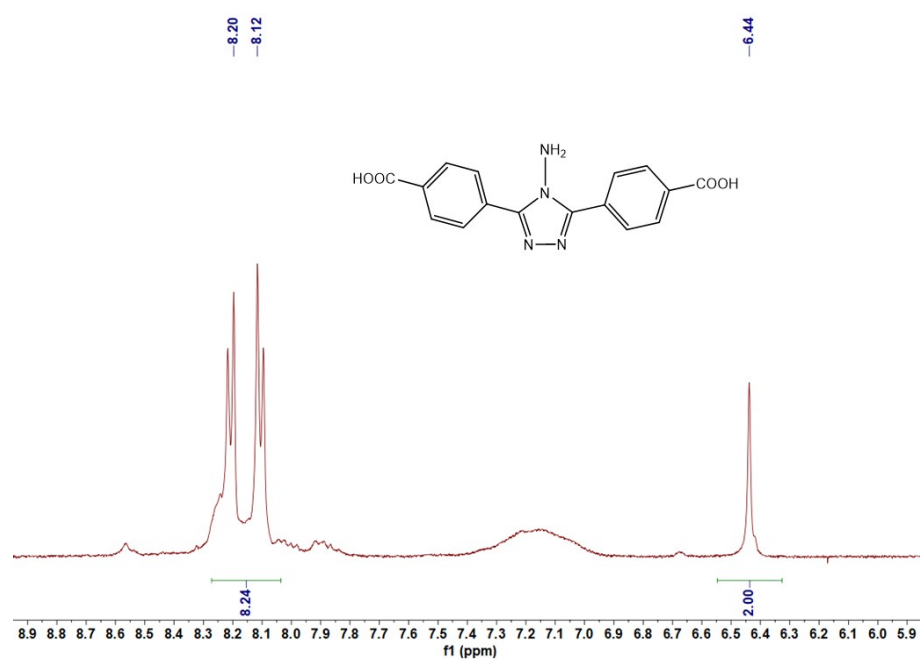


Fig. S14 ^1H NMR characterization of triazole dicarboxylic acid ligand

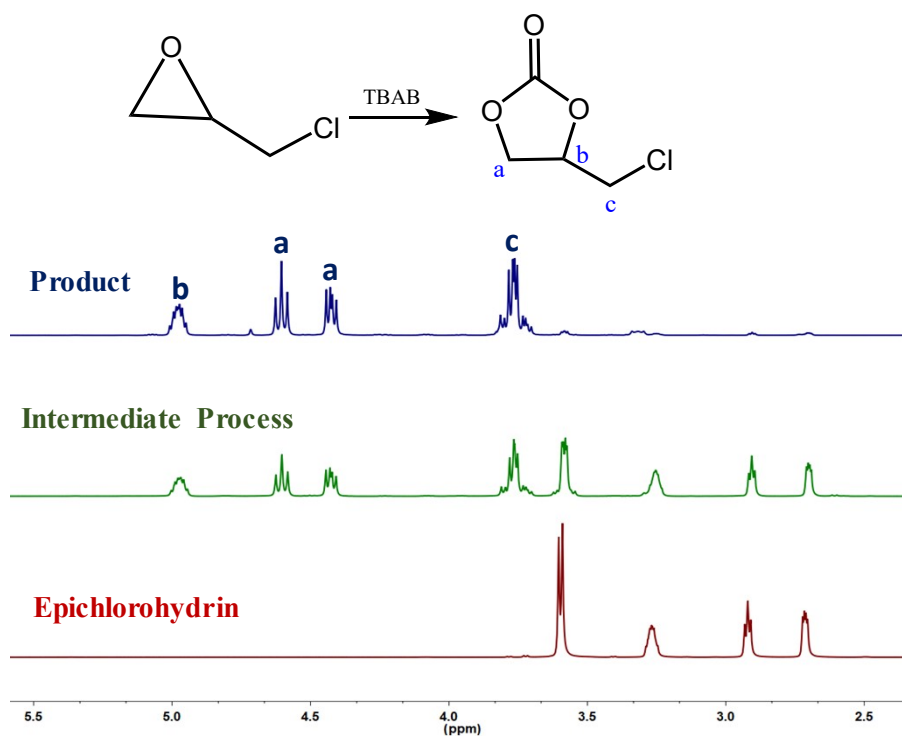


Fig. S15 X-ray powder diffraction characterization of Cu-MOF at different pH

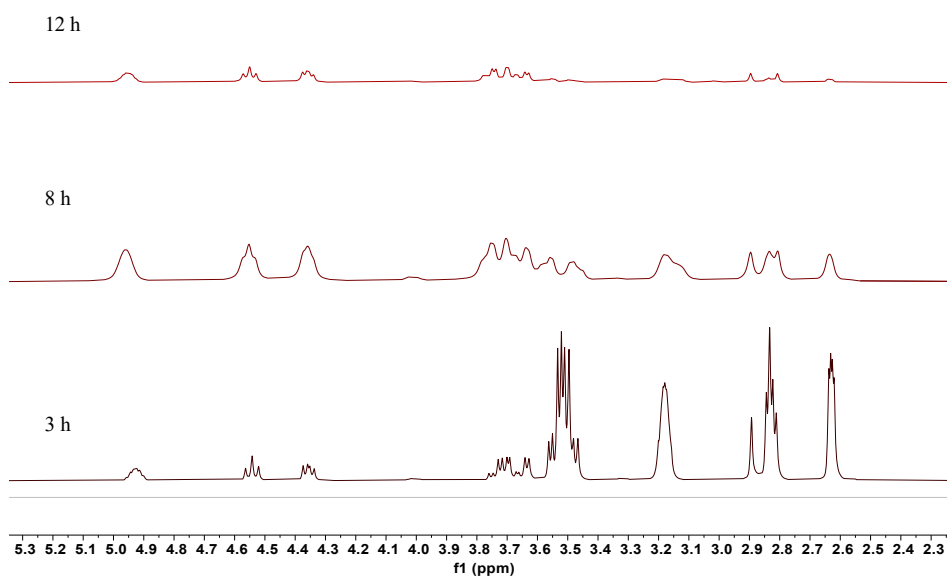


Fig. S16 ^1H NMR spectra of the conversion of epichlorohydrin at $90\text{ }^\circ\text{C}$ for different times

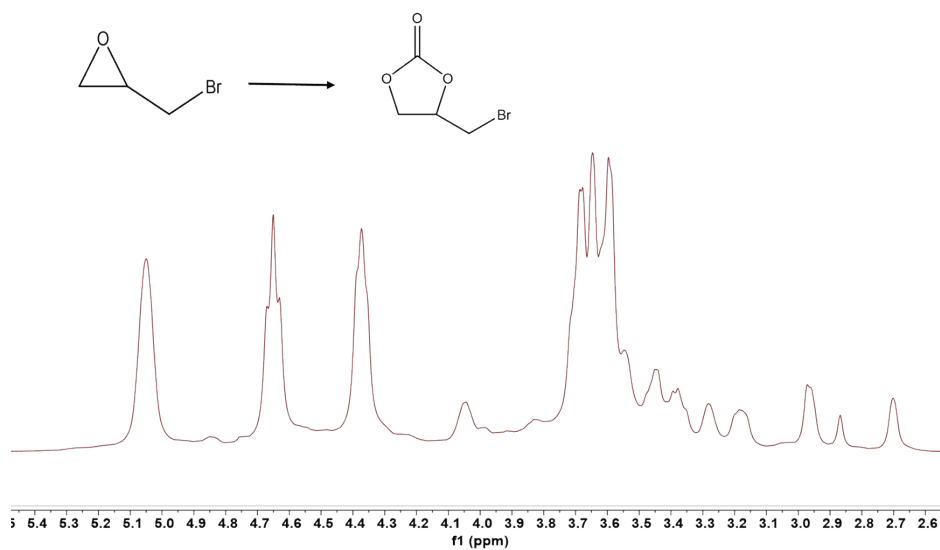


Fig. S17 Conversion of epoxypropyl bromide ¹H NMR spectrum

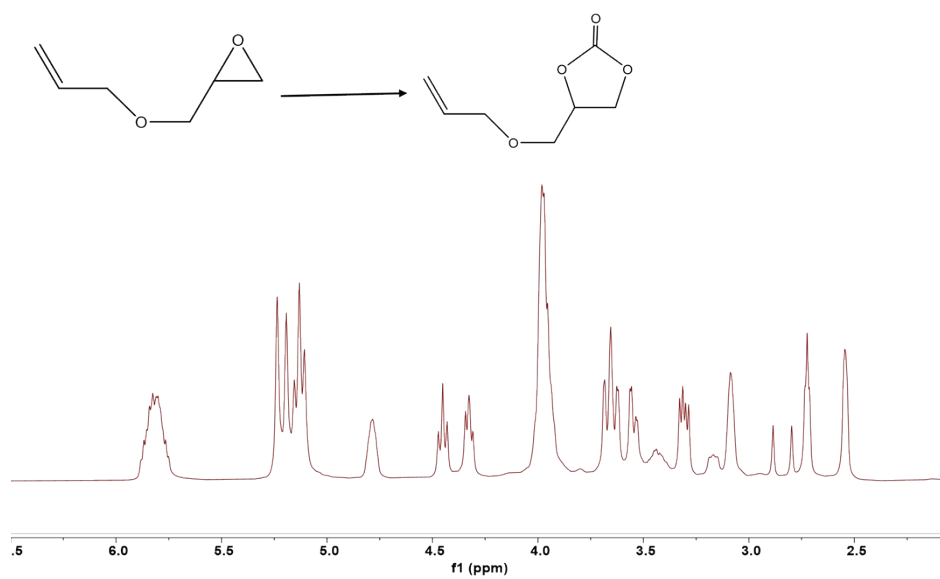


Fig. S18 Transformation of allyl glycidyl ether ¹H NMR spectrum

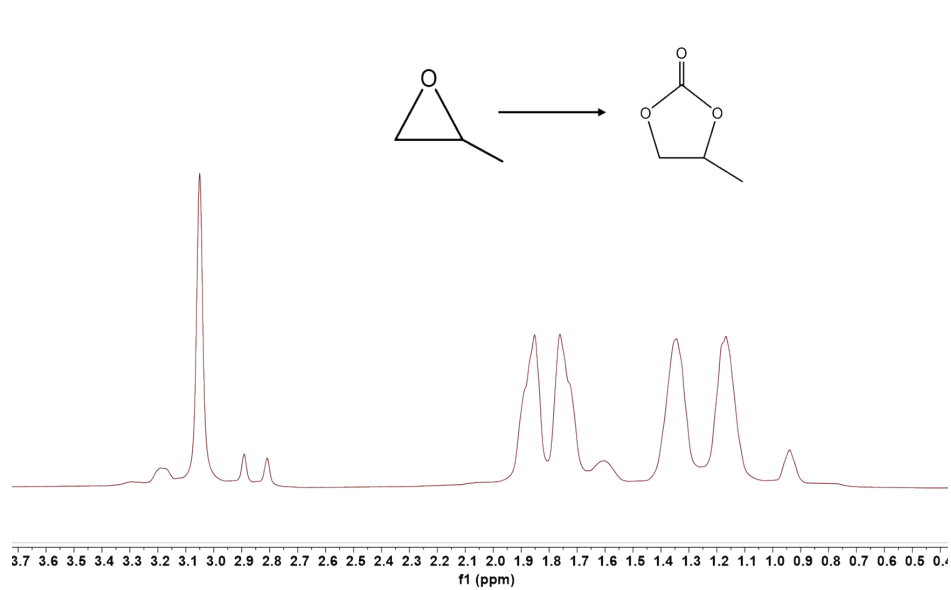


Fig. S19 Conversion of epoxypropane ¹H NMR spectrum

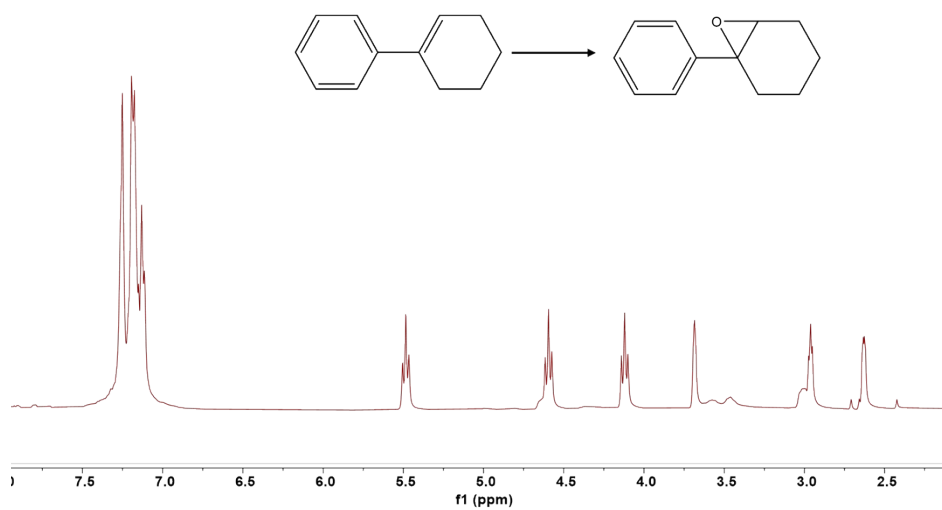


Fig. S20 Transformation of phenylcyclohexene ¹H NMR spectrum

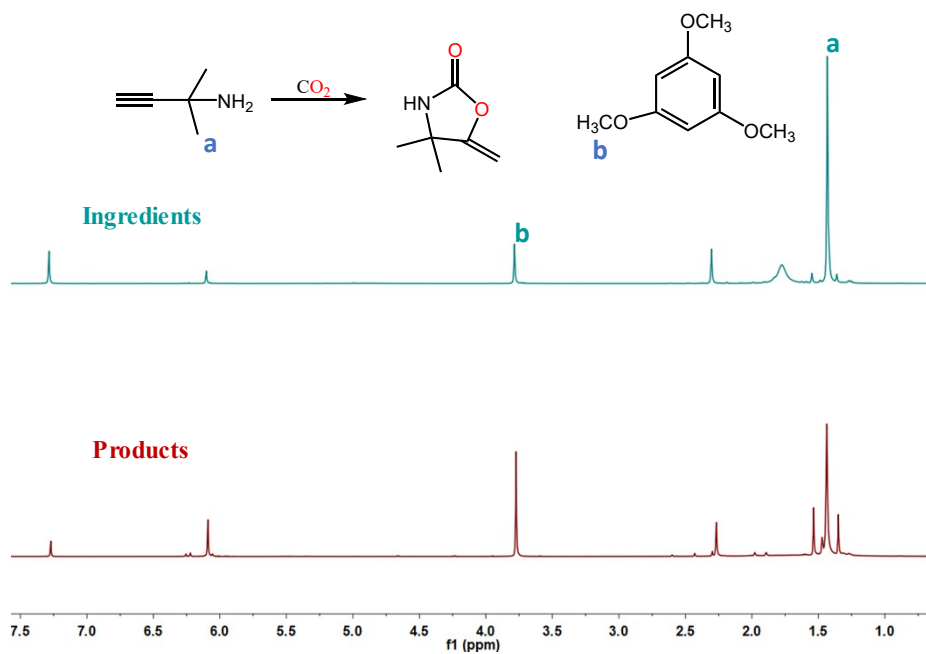


Fig. S21 ^1H NMR spectrum of the reaction of CO_2 with endoalkynylamine

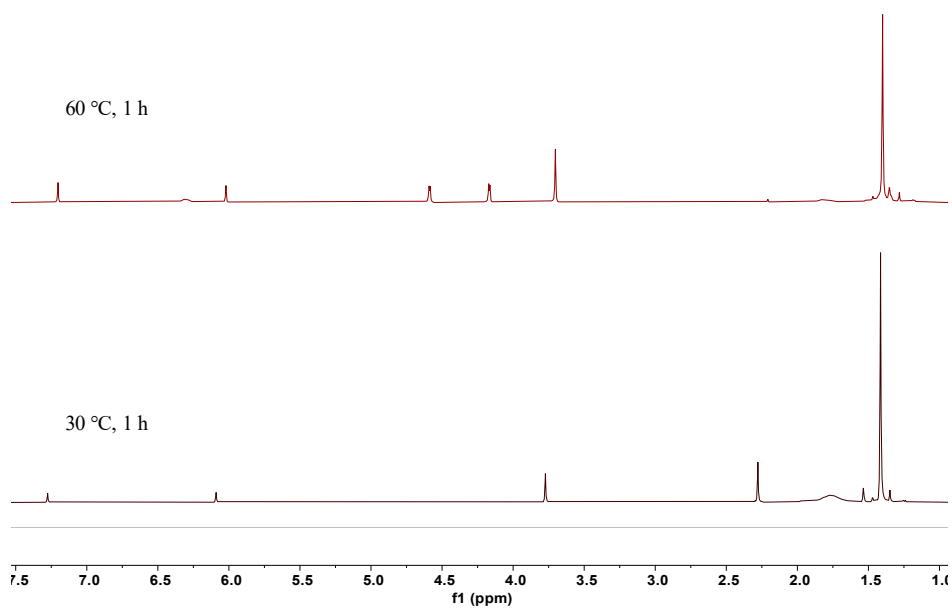


Fig. S22 Transformation of 2-methyl-3-butyne diamine at different temperatures ^1H NMR spectrum

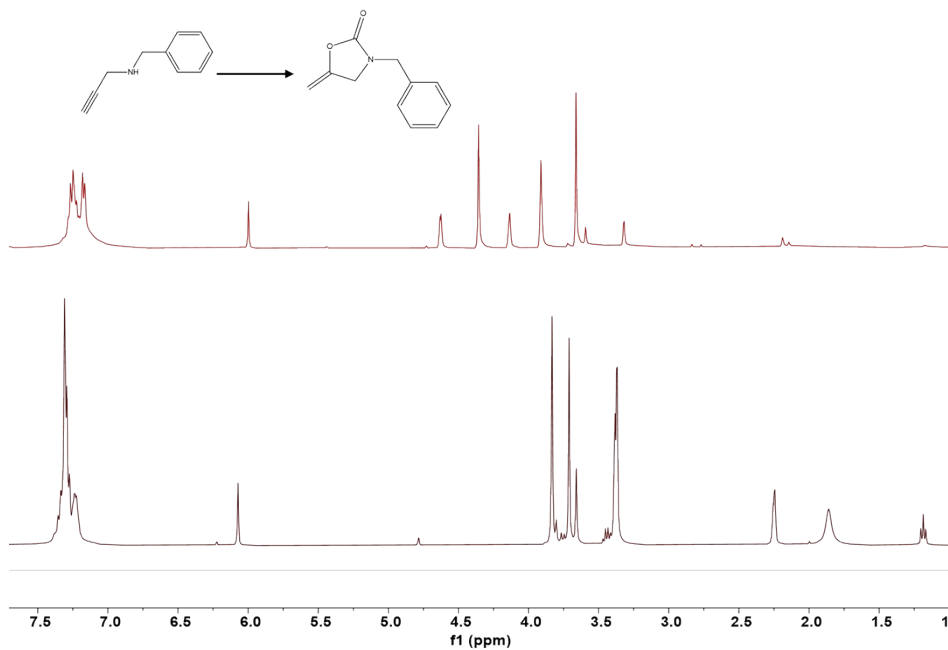


Fig. S23 Conversion of benzyl-2-propargylamine ¹H NMR spectrum

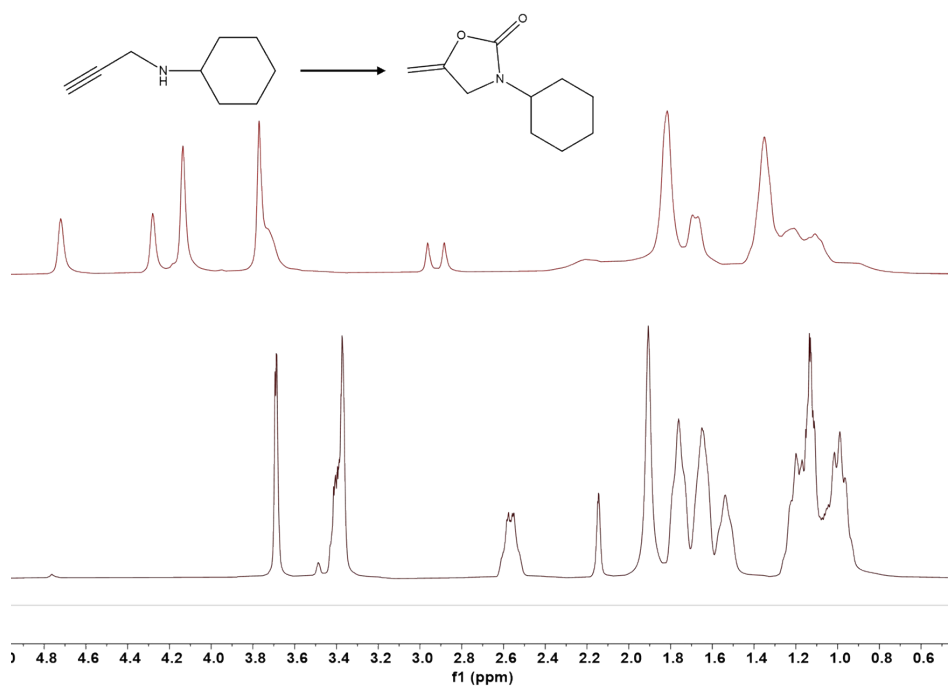


Fig. S24 Conversion of N-(prop-2-yn-1-yl)cyclohexanamine ¹H NMR spectrum

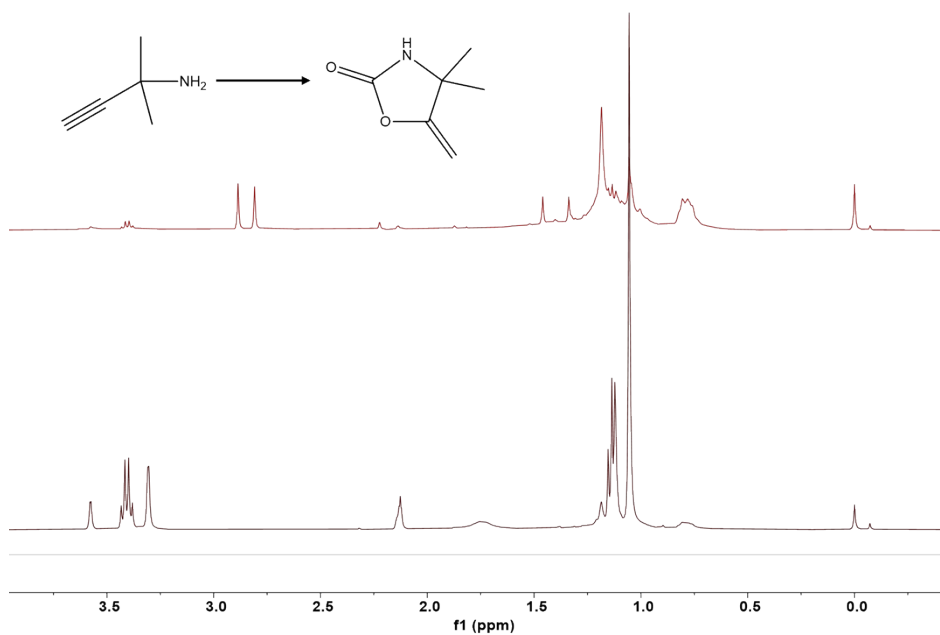


Fig. S25 Conversion of 2-methylbut-3-yn-2-amine ¹H NMR spectrum

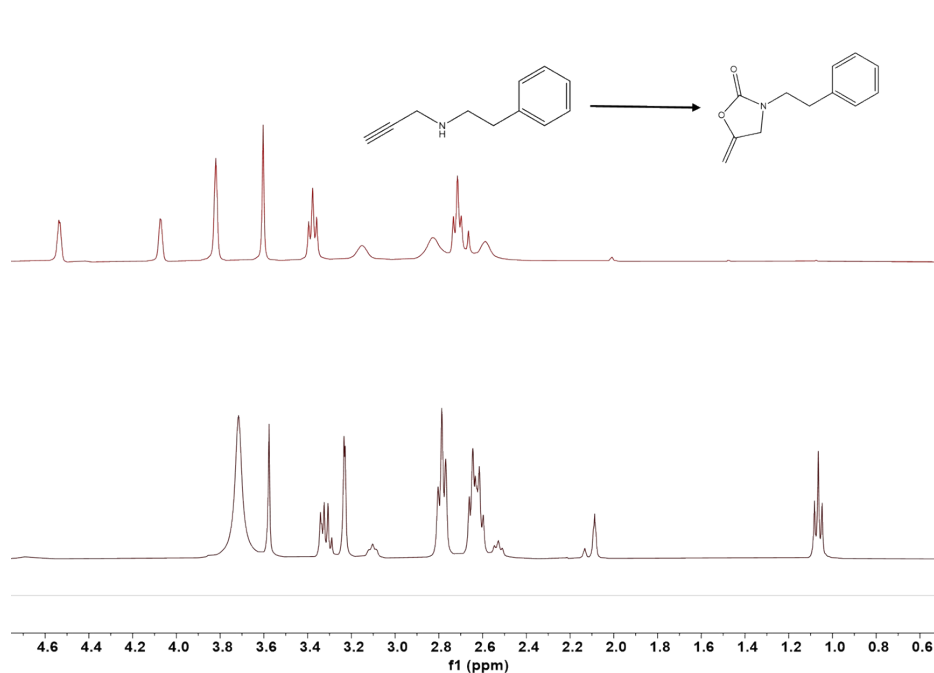


Fig. S26 Transformation of β-phenylethylamine ¹H NMR spectrum

Table S6 . The comparison of the TOF of other catalysts.

Catalyst	Additive/Solvent	T(°C)	P (atm)	t(h)	TOF(h ⁻¹)
This work ^[a]	--	60	1	1	15.8
SiO ₂ -TBD	--	90	80	21	0.84
CAT3	DMSO	60	1	10	0.79

HPG@[Au]	H ₂ O	RT	15	48	1.92
Fe ₄ O ₃ /[Au]	H ₂ O	RT	15	12	1.17
D301R	--	100	20	12	1.54
TOS-Ag ₈	DBU/CH ₃ CN	RT	1	24	4.13
PS-MimFeCl ₄	--	100	80	18	2.72
Ag-MOF-1	DBU/CH ₃ CN	RT	1	24	0.56
2Gn[TEG][Au]	H ₂ O	RT	1	24	1.77
ItBu	iPrOH	90	6	24	0.81
Pd(OAc) ₂	Toluene	20	40	24	0.71
TEOA	--	90	1	10	0.97
ZnCl ₂ (TBD) ₂	--	60	1	12	1.6

TOF: Turnover frequency was evaluated at optimal conditions and calculated by the mole number of product per mole number of catalytic active of Cu per hour.

[a] 1.3 mmol substrate, 0.057mmol catalyst, 1 atm CO₂, and solvent free. 1 h after the reaction, the yield determined by ¹H NMR with 1,3,5-Trimethoxybenzene as the internal standard.